Threading Polymer into Nanotubes: Evidence of Poly(ethylene oxide) Inclusion in Titanium Oxide

Maritza Volel* and Michel Armand

International Laboratory on Electroactive Materials, CNRS-UMR 2289, Université de Montréal, C.P. 6128, Succursale Centre-Ville, Montréal, Québec, H3C 3J7, Canada

Wladimir Gorecki

Laboratoire de Spectrométrie Physique, Université Joseph Fourier, 140 Avenue de la Physique, B.P. 87, 38402 Saint Martin d'Hères, France

Marie-Louise Saboungi

Centre de Recherche sur la Matière Divisée, CNRS-UMR 6619, 1B rue de la Férollerie, 45071 Orléans, Cedex 2, France

Received December 6, 2004. Revised Manuscript Received February 12, 2005

We introduce novel materials consisting of hydrated titanium oxide nanotubes filled with poly(ethylene oxide) (PEO) via a simple synthesis route. MAS NMR, TEM, TGA, PAS-FTIR, and ATR-FTIR measurements provide clear evidence of polymer inclusion in these nanotubes. PEO has been widely studied in the field of solid-state electrolytes, and its behavior in this confined environment shows unusual properties: faster relaxation times (as seen by PFGSE-NMR) and absence of transitions in DSC data, two criteria that hint of a potential enhancement of segmental mobility controlling ion diffusion. Conversely, the polymer serves as an efficient template when the inclusion compound is pyrolyzed to yield well-defined TiO_2 nanorods.

Introduction

Much interest has been aroused recently in the scientific community at large for the use of hybrid organic−inorganic materials,[1] for example, for catalysis, chiral synthesis, or enhancing optoelectronic properties.[2−4] Concurrently, several studies have been carried out on carbon−polymer[5,6] and intercalated[7−9] or dispersed polymer−clay composites to improve mechanical,[10,11] thermal, and transport properties.[12−15]

More specifically, the structure and dynamics of polymers in a confined environment[16,17] have shown that confinement constitutes an attractive approach to further the understanding and control of thermal properties such as the glass transition[18,19] and melting, which are closely coupled to transport properties[20,21] in these systems. Moreover, in the fast growing field of solid-state lithium batteries, transfer phenomena[22,23] at the polymer/electrode interface are often factors limiting either fluxes or lifetimes.

As a first approach to modeling this electrolyte/electrode interface on the nanoscale, we synthesized novel hybrid materials consisting of poly(ethylene oxide) (PEO) confined in the recently reported hydrated titanium oxide ($H_2Ti_3O_7$, trititanate) nanotubes.[24−27] We carried both in situ and ex

* To whom correspondence should be addressed. E-mail: maritza.volel@umontreal.ca.

(1) Langley, P. J.; Hulliger, J. *Chem. Soc. Rev.* **1999**, *28*, 279−291.
(2) Chen, W.-C.; Lee, S.-J.; Lee, L.-H.; Lin, J.-L. *J. Mater. Chem.* **1999**, *9*, 2999−3003.
(3) Wang, B.; Xi, H.-A.; Yin, J.; Qian, X.-F.; Zhu, Z.-K. *Synth. Met.* **2003**, *139*, 187−190.
(4) Zhang, J.; Wang, B.; Ju, X.; Liu, T.; Hu, T. *Polymer* **2001**, *42*, 3697−3702.
(5) Céspedes, F.; Alegret, S. *Trends Anal. Chem.* **2000**, *19*, 276−285.
(6) Dai, L.; He, P.; Li, S. *Nanotechnology* **2003**, *14*, 1081−1097.
(7) Lemmon, J. P.; Wu, J.; Oriakhi, C.; Lerner, M. M. *Electrochim. Acta* **1995**, *40*, 2245−2249.
(8) Krishnamoorti, R.; Vaia, R. A.; Giannelis, E. P. *Chem. Mater.* **1996**, *8*, 1728−1734.
(9) Anastasiadis, S. H.; Karatasos, K.; Vlachos, G.; Manias, E.; Giannelis, E. P. *Phys. Rev. Lett.* **2000**, *84*, 915−918.
(10) Ahmad, Z.; Sarwar, M. I.; Wang, S.; Mark, J. E. *Polymer* **1997**, *38*, 4523−4529.
(11) Nowaczyk, G.; Glowinkowski, S.; Jurga, S. *Solid State Nucl. Magn. Reson.* **2004**, *25*, 194−199.
(12) Croce, F.; Appetecchi, G. B.; Persi, L.; Scrosati, B. *Nature* **1998**, *394*, 456−458.
(13) Adebahr, J.; Byrne, N.; Forsyth, M.; MacFarlane, D. R.; Jacobsson, P. *Electrochim. Acta* **2003**, *48*, 2099−2103.
(14) Strümpler, R.; Glatz-Reichenbach, J. *J. Electroceram.* **1999**, *3*, 329−346.
(15) Zhou, J.; Fedkiw, P. S. *Solid State Ionics* **2004**, *166*, 275−293.
(16) Schönhals, A.; Goering, H.; Schick, C. *J. Non-Cryst. Solids* **2002**, *305*, 140−149.
(17) Venuti, V.; Crupi, V.; Galli, G.; Majolino, D.; Migliardo, P. *J. Mol. Struct.* **2002**, *615*, 83−88.
(18) Schüller, J.; Mel'nichenko, Y. B.; Richert, R.; Fischer, E. W. *Phys. Rev. Lett.* **1994**, *73*, 2224−2227.
(19) Zeng, Y.; Shi, Y.; Chen, G. *Physica A* **2003**, *319*, 80−98.
(20) Vorrey, S.; Teeters, D. *Electrochim. Acta* **2003**, *48*, 2137−2141.
(21) Wu, J.; Gross, A. F.; Tolbert, S. H. *J. Phys. Chem. B* **1999**, *103*, 2374−2384.
(22) Orsini, F.; Du Pasquier, A.; Beaudoin, B.; Tarascon, J. M.; Trentin, M.; Langenhuizen, N.; De Beer, E.; Notten, P. *J. Power Sources* **1998**, *76*, 19−29.
(23) Tarascon, J. M.; Armand, M. *Nature* **2001**, *414*, 359−367.
(24) Kasuga, T.; Hiramatsu, M.; Hoson, A.; Sekino, T.; Niihara, K. *Adv. Mater.* **1999**, *11*, 1307−1311.
(25) Du, G. H.; Chen, Q.; Che, R. C.; Yuan, Z. Y.; Peng, L.-M. *Appl. Phys. Lett.* **2001**, *79*, 3702−3704.
(26) Wang, Y. Q.; Hu, G. Q.; Duan, X. F.; Sun, H. L.; Xue, Q. K. *Chem. Phys. Lett.* **2002**, *365*, 427−431.

10.1021/cm047880r CCC: $30.25 © 2005 American Chemical Society
Published on Web 03/17/2005

situ generation of the hybrids: either by allowing the polymer to be wrapped by the tubes while they are being formed in aqueous medium (the nanotubes are believed to be generated by a scrolling of the titanium oxide planes),[26,27] or by contacting already synthesized empty tubes with a solution of the polymer. Both approaches were successful as confirmed by TEM, TGA, MAS NMR, PAS-FTIR, and ATR-FTIR analysis. We also addressed the dynamics of these systems through DSC and PFGSE-NMR studies. The measurement of the decay curves with T_1 (spin−lattice) and T_2 (spin−spin) relaxation time constants for the bulk and the confined polymers allowed us to compare the respective time scales of these dynamics.

Experimental Section

Synthesis. TiF_4 99.9% (Aldrich) was used as the titanium oxide precursor. A 0.04 M aqueous solution of TiF_4 was prepared. The pH of the as-prepared solution was around 1.9, an adequate pH for the homogeneous precipitation of anatase TiO_2 at 60 °C.[28] 100 mL of this solution was poured into a series of sealed Teflon vials containing various amounts of PEO (M_w 5 × 10^6, Aldrich) to give weight percents of PEO to TiF_4 of 0% (blank sample), 10%, 20%, and 30%. The PEO-containing samples were allowed to become homogeneous by a complete dissolution of the PEO in the TiF_4 aqueous solutions at room temperature. All samples were then placed into an oven at 60 °C for 24 h for precipitation of plain TiO_2 and TiO_2−PEO hybrids to occur. The precipitated TiO_2 was in the form of anatase as confirmed by X-ray diffraction analysis. The titanium oxide nanotubes were generated by following the procedure described by Kasuga and co-workers.[24] A 10 M aqueous NaOH (pellets from Aldrich) solution was poured onto a few milligrams of the respective plain TiO_2 and TiO_2−PEO hybrids inside a homemade assembly consisting of a sealed Teflon vial slid into a sealed stainless steel vessel. The whole system was then heated at 110 °C for 24 h. After cooling to room temperature, the generated plain nanotubes and the respective PEO hybrids (resulting from the resistance of PEO to these highly basic conditions) were isolated by centrifuging at 7000 rpm for 15 min. A series of washings with water each followed by centrifuging and isolating were made until a neutral pH was reached. The compounds were then finally rinsed with methanol (Aldrich), isolated, and dried at 60 °C for 24 h.

For the ex-situ generation of a hybrid, a few milligrams of plain nanotubes were placed into an aqueous homogeneous gel of PEO (5×10^6) consisting of 0.5 g of PEO dissolved in 100 mL of water. The nanotubes were dispersed in the gel by placing the mixture in an ultrasonic bath for 30 min. The system was then allowed to rest for 48 h for the PEO to impregnate the nanotubes. The hybrid was then isolated after centrifuging and rinsing three times with water and one time with methanol. The compound was finally dried at 60 °C for 24 h.

TEM. All samples were imaged with a Philips CM-20 transmission electron microscope equipped with a LaB_6 crystal for electron generation. A few milligrams of each sample were suspended in methanol, and the solution was dispersed by sonication for 5 min. A drop of this solution was then placed on a TEM grid (copper grid covered by electric arc-deposited carbon) and allowed to dry in air under a lamp. For image acquisition, the applied voltage was set between 80 and 200 kV.

MAS NMR. A Bruker DSX-300 solid-state nuclear magnetic resonance spectrometer operating at 7 T was used. ^{1}H (resonance frequency: 300.18 MHz) solid-state NMR spectra consisting of at least 8000 points and four co-added scans within a spectral window of 10 kHz were acquired for each sample. A Bloch decay experiment with magic angle spinning (magic angle, 54.7°; spin rate, 12 kHz), with an impulse of 90° for 4.5 μs, was performed.

PAS-FTIR. We used a Bio-Rad FTS 6000 spectrometer equipped with a ceramic IR source and a photoacoustic detector. For each sample, a spectrum consisting of 128 co-added scans with a resolution of 4 cm^{-1} was acquired in the rapid scan mode with a speed of 2.5 kHz. A background done on carbon black under the same conditions was subtracted from the spectra.

ATR-FTIR. Each spectrum was acquired on a Nicolet Nexus 870 spectrometer equipped with an attenuated total reflectance cell (ATR Smart ARK accessory) with a ZnSe window, a XT-KBr beam splitter, and a DTGS-TEC detector. The samples were placed directly on the ZnSe window, and the spectra were recorded with a resolution of 4 cm^{-1} and averaged over 128 scans from which a background was subtracted. The spectra were Fourier transformed and processed with a Happ−Genzel apodization function and a Mertz phase correction.

DSC/TGA. A Pyris 1 Perkin-Elmer differential scanning calorimeter was used. Each sample (∼2.5 mg) was crimp-sealed in an aluminum pan and scanned at 5 °C/min from 20 to 120 °C. The melt was then quenched at 500 °C/min from 120 to −150 °C, and a second scan was then done at 5 °C/min from −150 to 120 °C. TGA analysis was carried out by a Perkin-Elmer TGA 7 thermogravimetric analyzer. Each sample (∼2.5−6 mg) was placed in a platinum pan and heated in a furnace under nitrogen flow between 20 and 800 °C at a rate of 10 °C/min.

PFGSE-NMR. A homemade spectrometer equipped with a superconducting coil providing a direct magnetic field of 6.6 T was used. For the blank PEO samples, we applied a pulsed magnetic field gradient technique (PMFG) with spin−echo (SE) using the pulse sequence ($\pi/2$, τ, π) described by Stejskal and Tanner.[29] The ^{1}H free induction decay (FID) curve in the XY plane, due to transverse (or spin−spin) relaxation with a characteristic time (T_2), was reconstructed by measuring the amplitude of the echo signal for different τ values at a temperature of 360 K. The measured echo amplitude ($A(2\tau)$), for each τ value, was normalized to the maximum intensity at $\tau = 0$. Due to the high crystallinity of the hybrid samples, no echo signal was observed. In those cases, the free induction decay curve was directly generated by applying a $\pi/2$ pulse and allowing the magnetic moments to relax over time.

The longitudinal (or spin−lattice) relaxation time (T_1) was estimated by applying a (π, τ, $\pi/2$) sequence and measuring the magnetization on the Z axis (M_z) for different τ values. The decay of $M_0 - M_z$ as a function of τ is proportional to T_1, M_0 being the measured magnetization for $\tau = 1$ s. More details on these types of measurements can be found elsewhere.[30]

Results and Discussion

By examining Figure 1, we can tell from the morphologies of plain trititanate nanotubes (Figure 1a) as compared to those prepared in the presence of various amounts of polymer (Figure 1b−e) that the polymer has a marked influence on the titanium oxide structure. In the case of pristine trititanate, the tubular structure is well defined, whereas in the presence

(27) Chen, Q.; Du, G. H.; Zhang, S.; Peng, L.-M. *Acta Crystallogr.* **2002**, *B58*, 587−593.
(28) Shimizu, K.; Imai, H.; Hirashima, H.; Tsukuma, K. *Thin Solid Films* **1999**, *351*, 220−224.
(29) Stejskal, E. O.; Tanner, J. E. *J. Chem. Phys.* **1965**, *42*, 288−292.
(30) Gorecki, W.; Jeannin, M.; Belorizky, E.; Roux, C.; Armand, M. *J. Phys.: Condens. Matter* **1995**, *7*, 6823−6832.

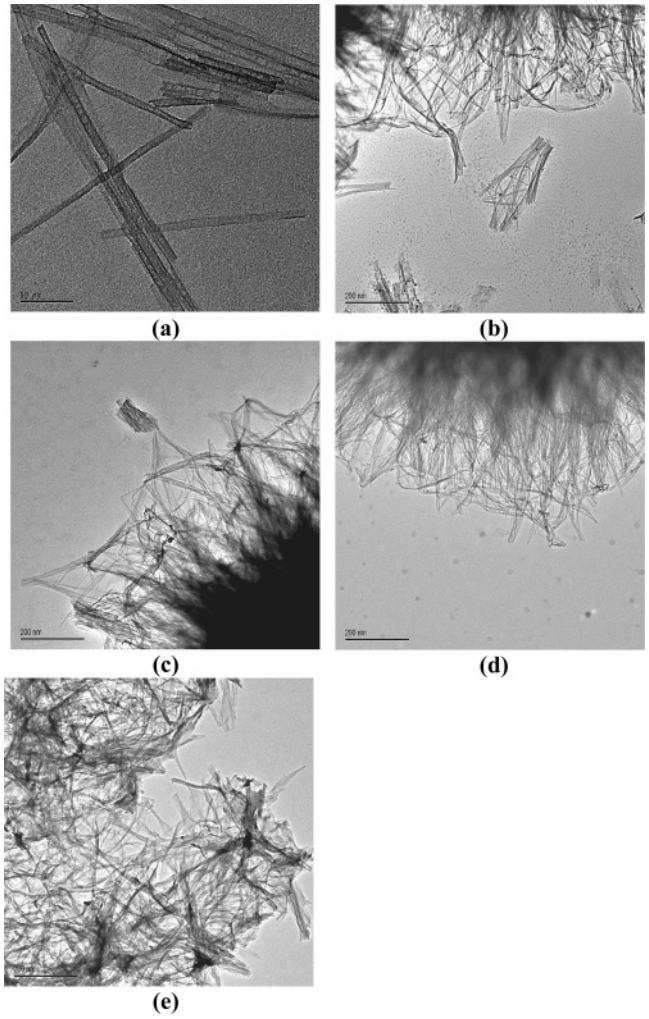

Figure 1. TEM images of the samples: (a) plain titanium oxide nanotubes, (b) 10% PEO, (c) 20% PEO, (d) 30% PEO, and (e) X PEO.

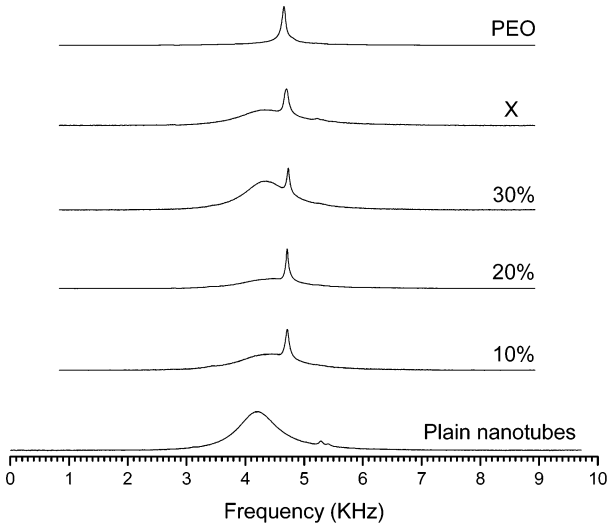

Figure 2. MAS NMR of the hybrid PEO−titanium oxide samples versus PEO and plain nanotubes.

of PEO, folding of the titanium oxide scroll is incomplete in some areas.

Proton MAS NMR data (Figure 2) revealed the presence of two types of protons: hydroxyl protons associated with the oxide surface of the trititanate structure,[27] and aliphatic protons from PEO. In fact, the polymer can provide strong hydrogen bonding between ether oxygens and acidic surface protons of the trititanate structure. Water, if present, is believed to be confined but to exchange rapidly with the hydroxyl protons and be part of the broad "inorganic" protons peak. We suggest that during synthesis (see Experimental Section) PEO bonds to the initially formed trititanate sheets (during the thermal treatment in the presence of the strong base), which in turn confine the polymer to the medullar space when the scrolling process[26] takes place, leading to a multiwalled tube.[27]

PAS-FTIR spectra (Figure 3a) show the O−H stretching mode around 3400 cm^{-1} for all compounds. Around 1650 cm^{-1} it is also possible to see H−O−H bending modes that confirm the hydrogen bonding in the structures and/or water. PEO has been reported to form a stable complex with water involving 3 molecules of water per ethylene oxide unit.[31] Bands for plain PEO are barely apparent for the hybrid samples, corroborating the idea that PEO is trapped inside the tube scroll. By zooming in the region between 2700 and 3000 cm^{-1} (Figure 3b), it is possible to see for the hybrid compounds the C−H (from the aliphatic CH_2 in the ethylene oxide units) symmetric and asymmetric stretch modes, at 2850 and 2920 cm^{-1}, respectively. These bands are similar to those observed, for instance, in self-assembled monolayers.[32] These C−H stretch modes are less pronounced for the sample designated as X, which was brought into contact with PEO after the synthesis of empty trititanate tubes. We hypothesize that the PEO is only allowed to enter the hollow center of the scroll as evidenced by the surface-sensitive ATR-FTIR spectra where no bands could be detected for PEO at the surface of the hybrid samples (Figure 3c). For the in-situ preparation, higher contents of imperfect scrolling regions leave more "IR accessible" PEO as detected by bulk-sensitive PAS-FTIR. PEO is unlikely to intercalate between the layers of $H_2Ti_3O_7$. Although reminiscent of the clay structures with intercalated polyethers,[7−9] the density of OH groups in the interlayer space (0.78 nm) is much higher, implying strong plane-to-plane hydrogen bonding.[27] The trititanate is not known to form adducts from propping up the layers.

TGA data (Figure 4) show that PEO is totally decomposed into volatile components around 400 °C (Figure 4a). On the other hand, the dehydration of $H_2Ti_3O_7$ to give TiO_2 corresponds to ∼7% weight loss. The pristine nanotubes lose ∼21%, and thus 14% is accountable for water, tightly held in the tubes, whose loss occurs concomitantly with the $2OH_{surface} \rightleftharpoons O_{surface} + H_2O$ condensation reaction. As can be seen, the amount of polymer present initially for the in-situ procedure does influence the weight loss, but not proportionally. When the polymer replaces the "pipe" water, it is now possible to see a knee between 300 and 350 °C (Figure 4b). This change in regime is likely due to an accelerated polymer fragmentation, catalyzed by the surface OH groups, becoming increasingly acidic with dehydration

(31) Graham, N. B.; Zulfiqar, M.; Nwachuku, N. E.; Rashid, A. *Polymer* **1990**, *31*, 909−916.
(32) Nuzzo, R. G.; Dubois, L. H.; Allara, D. L. *J. Am. Chem. Soc.* **1990**, *112*, 558−569.

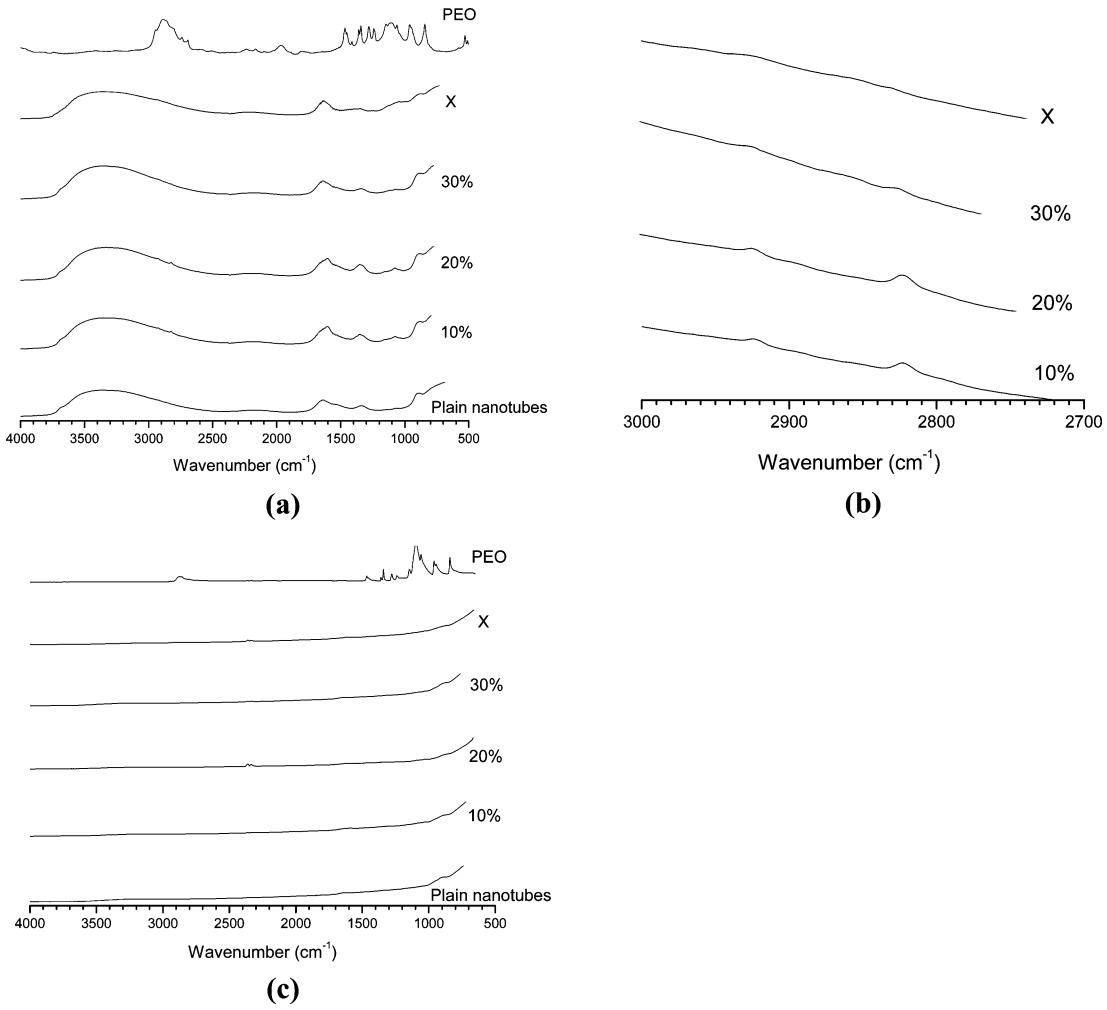

Figure 3. PAS-FTIR of (a) hybrid PEO−titanium oxide samples versus PEO and plain nanotubes; (b) hybrid samples, zoom in of a specific spectral region; and (c) ATR-FTIR spectra of all samples.

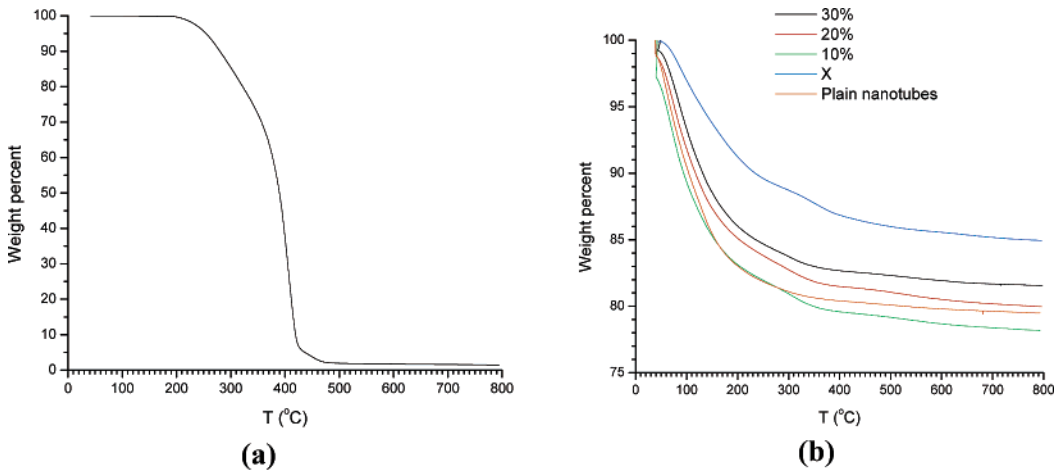

Figure 4. TGA of (a) PEO and (b) hybrid PEO−titanium oxide and plain nanotubes.

and temperature. Ethers are known for their sensitivity to depolymerization via oxonium formation. Dioxane is the main product formed from PEO. The global weight loss tendency seems to be less pronounced for the samples containing increased amounts of polymer. The fact that PEO can allow hydrogen bonding favors water retention, leading to a more gradual water weight loss. In the case of tubes containing less polymer, more water molecules can be incorporated into the tubes, and at the same time this water is free to evaporate, so that a steeper water weight loss occurs.

Interestingly, TEM analysis of the samples after TGA up to 800 °C reveals new morphologies (Figure 5). The nanotubes of Figure 1 are now converted into TiO_2 compact nanorods (Figure 5), except for the ex-situ hybrid that generates disrupted structures. Surprisingly, for the incompletely folded structures observed in the in-situ samples (Figure 1b−d), the final shape is a rodlike feature (Figure

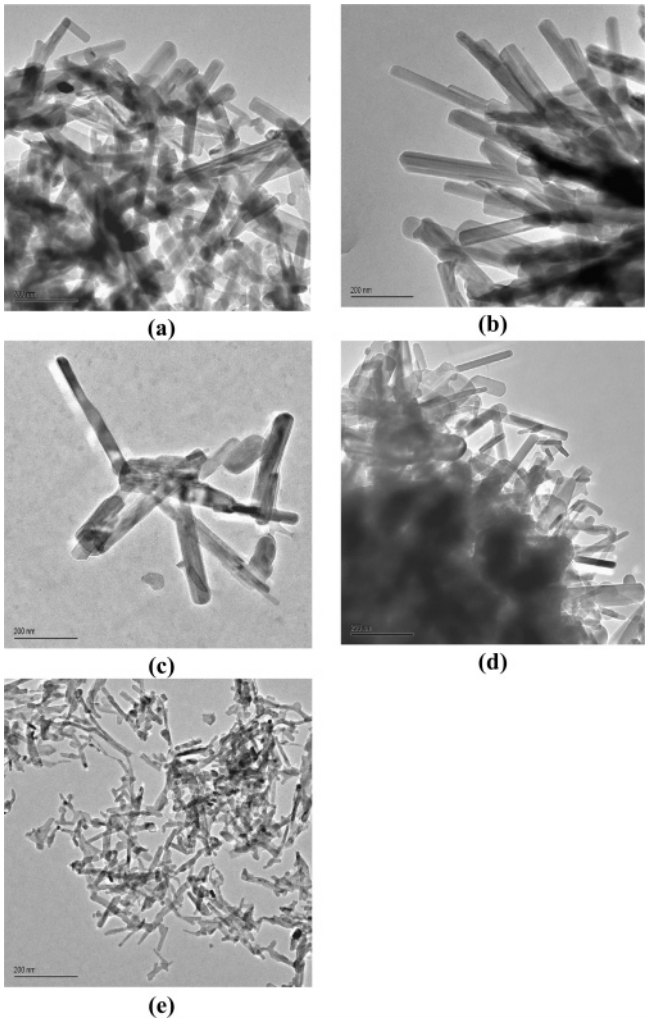

Figure 5. TEM images of the samples after TGA up to 800 °C: (a) plain titanium oxide nanotubes, (b) 10% PEO, (c) 20% PEO, (d) 30% PEO, and (e) X PEO.

5b−d), implying that the polymer strands act as a transient template to allow the dehydration process to maintain the initial aspect ratio of perfectly scrolled empty tubes. For the ex-situ sample, containing less incompletely folded regions, it is more difficult for the polymer degradation products to escape, resulting in bursting. The imperfect tubes obtained from the in-situ synthesis are more permeable and thus allow the volatile products to escape progressively. This is, to our knowledge, the first report of titania nanorod synthesis[33−37] from nanotubes, using a polymer template that affects the transformation. The TiO_2 nanorods could be of interest for light harvesting[38] and are susceptible to be topochemically transformed into the well-known electrode material $Li_4Ti_5O_{12}$[39] by reaction with LiOH or Li_2CO_3 and subsequent heating to high temperatures for several hours.

From the DSC data, no transitions, due to a confinement[16−21] of the polymer, could be observed. However, the very small size of the samples (∼2.5 mg) is borderline in terms of detection limit, and the polymer content of our samples (up to 30%) is small as opposed to the case of oxide additives dispersed in polymers[15] where the polymer makes at least 80% w/w of the sample.

To further investigate the confinement effect, we turned to NMR, and more specifically to the proton PFGSE-NMR measurements of relaxation times. As a first approach, we measured the ^{1}H decay curves, with T_1 (spin−lattice) and T_2 (spin−spin) time constants, for plain PEO and the in-situ generated hybrids (Figures 6 and 7). From Figure 6, it is possible to see that the free induction decay (FID) curve for free PEO (Figure 6a) drops to zero following an exponential decay over a time scale in the range of 20 ms, whereas for the confined samples (Figure 6b) the scale drop is in the range of 500 μs. Roughly, the relaxation dynamics in the confined samples are about 40 times faster than for the free PEO. Moreover, the free induction decay is faster for the sample containing 30% weight PEO, and then, in increasing order of time, we find the 20% and 10% weight samples. Intuitively, we would expect the opposite because more polymer means less possible confinement by the titanium oxide matrix. One explanation for this behavior could be that the less polymer introduced in the sample, the smaller the population of polymer molecules in each tube; therefore, each polymer molecule is more likely to be able to move freely as compared to the other case (more polymer) where it would be sterically hindered by its neighbors thus leading to faster relaxation times. We see likely a maximum effect on the chain dynamics at 30%, probably a tradeoff between the confinement by more polymer neighbors (causing faster chain dynamics) and the strong interactions of the polymer with the surface TiOH.

The magnetization decay along the Z axis (Figure 7) shows again a slower relaxation processes for the free PEO (Figure 7a) as compared to the confined samples (Figure 7b), roughly by a factor of 4 on the time scale. A similar tendency to the FID curves (Figure 6b) is observed for the magnetization decay as a function of polymer concentration (Figure 7b). One interesting phenomenon is that it is possible to see that the exponential decays have two regimes or, more accurately, a distribution between two extremes: the first one is a drastic drop before 10 ms and the second one a smooth decay over 240 ms. We attribute the slower regime to the amount of polymer away from the surface (i.e., closer to the center of the tube cavity), where it is confined but with dipolar interactions from its neighbors that are weaker to those that are experienced by the amount of polymer that is chemisorbed via hydrogen bonds on the inner walls of the tubes. The faster regime is therefore associated with the latter that is expected to be relatively immobile (except for local segmental and/or rotational dynamics), leading to a faster decay of the magnetization along the Z axis.

(33) Pradhan, S. K.; Reucroft, P. J.; Yang, F.; Dozier, A. *J. Cryst. Growth* **2003**, *256*, 83−88.
(34) Nad, S.; Sharma, P.; Roy, I.; Maitra, A. *J. Colloid Interface Sci.* **2003**, *264*, 89−94.
(35) Wu, J.-M. *J. Cryst. Growth* **2004**, *269*, 347−355.
(36) Miao, L.; Tanemura, S.; Toh, S.; Kaneko, K.; Tanemura, M. *J. Cryst. Growth* **2004**, *264*, 246−252.
(37) Armstrong, A. R.; Armstrong, G.; Canales, J.; Bruce, P. G. *Angew. Chem., Int. Ed.* **2004**, *43*, 2286−2288.
(38) Kay, A.; Grätzel, M. *Sol. Energy Mater. Sol. Cells* **1996**, *44*, 99−117.
(39) Nakahara, K.; Nakajima, R.; Matsushima, T.; Majima, H. *J. Power Sources* **2003**, *117*, 131−136.

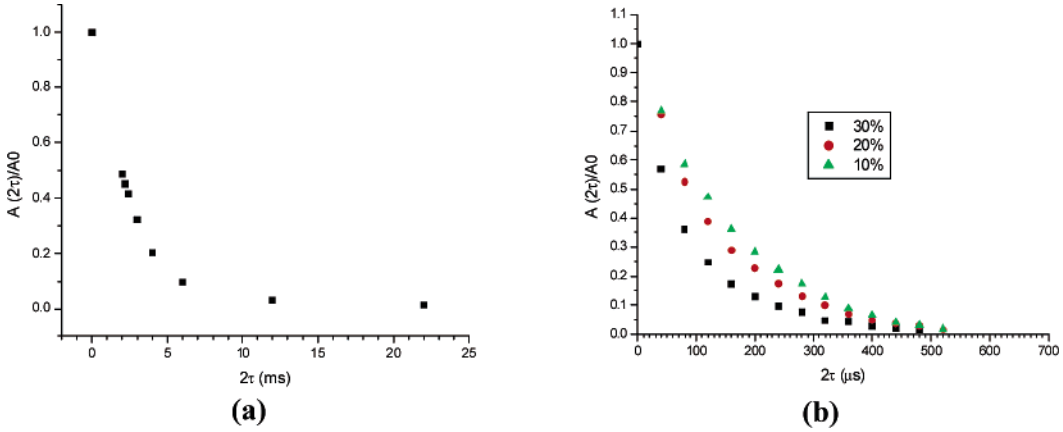

Figure 6. [1]H free induction decay, with a time constant T_2, as measured by PFGSE-NMR for: (a) plain PEO and (b) hybrid PEO−titanium oxide nanotubes.

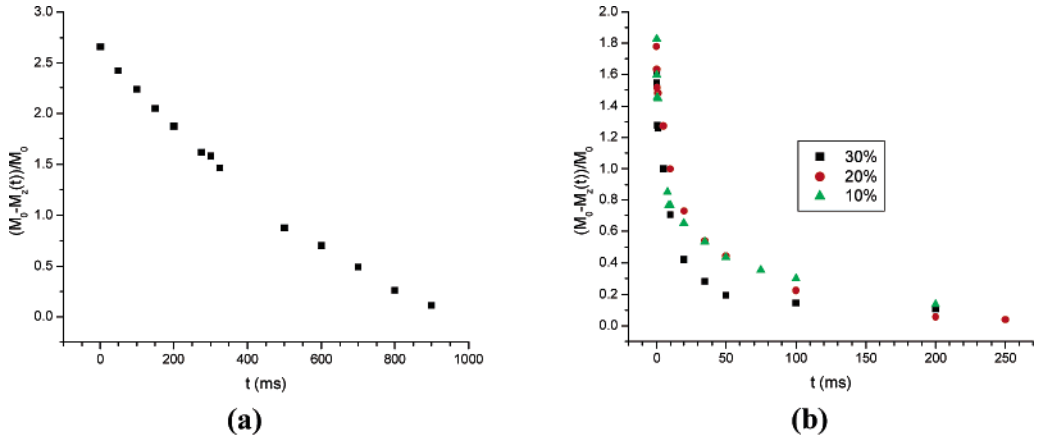

Figure 7. [1]H magnetization decay, with a time constant T_1, as measured by PFGSE-NMR for: (a) plain PEO and (b) hybrid PEO−titanium oxide nanotubes.

Conclusions

Successful confinement of PEO into a titanium oxide matrix was achieved. To our knowledge, this is the first time that polymers are thread into nanotubes. The fact that the polymer can enter the already scrolled trititanate indicates a strong affinity between the ether oxygens and the OH groups lining the inner cavity. The confined polymer presents faster relaxation dynamics than the bulk material. If this system is viewed as a nanoscale mimic of the electrode/polymer electrolyte interface (as found in lithium batteries), the faster relaxation dynamics implies faster local segmental and/or rotational polymer motions and would favor enhanced ionic transport.[40] The effect seems to be larger than the "inverse" configuration in which ceramic nanoparticles are dispersed in a PEO matrix.[12,15,41] Our findings may eventually translate into practical improvements of the transfer kinetics at this poorly mastered electrode/electrolyte interface. Also, the transformation from nanotubes to nanorods only in the presence of the polymer is novel and, although not fully understood, significant for designing new nanomaterials. Further work will emphasize neutron studies to probe the improvement on structure and kinetics, thus obtained, and NMR studies following lithium salt complexing with the confined PEO.[42,43]

Acknowledgment. We are grateful to the French government, through Madame Dominique Sotteau from the General Consulate of France in Montréal, for providing an EGIDE scholarship to M.V. for experiments at the Centre de Recherche sur la Matière Divisée in Orléans and at the Université Joseph Fourier in Grenoble. Special thanks are due to Dr. Cédric Malveau for MAS NMR experiments. The work in France was supported by a special grant from the Region Centre, Orléans.

CM047880R

(40) Volel, M.; Gorecki, W.; Armand, M. *Macromolecules* **2004**, *37*, 8373−8380.
(41) Bloise, A. C.; et al. *Electrochim. Acta* **2001**, *46*, 1571−1579.
(42) Mao, G.; Fernandez Perea, R.; Howells, W. S.; Price, D. L.; Saboungi, M.-L. *Nature* **2000**, *405*, 163−165.
(43) Mao, G.; Saboungi, M.-L.; Price, D. L.; Armand, M. B. *Phys. Rev. Lett.* **2000**, *84*, 5536−5538.